



**HAL**  
open science

## Synthesis, characterization and luminescent properties of Sr<sub>1-x</sub>Pb<sub>x</sub>WO<sub>4</sub> solid solution (x=0, 0.5 and 1)

A. Hallaoui, A. Taoufyq, B. Bakiz, F. Guinneton, J-C Valmalette, Sylvie Villain, Madjid Arab, A. Benlhachemi, L. Bazzi, Jean-Raymond Gavarri

► **To cite this version:**

A. Hallaoui, A. Taoufyq, B. Bakiz, F. Guinneton, J-C Valmalette, et al.. Synthesis, characterization and luminescent properties of Sr<sub>1-x</sub>Pb<sub>x</sub>WO<sub>4</sub> solid solution (x=0, 0.5 and 1). XII MAGHREB DAYS OF MATERIAL SCIENCES, 2017, Unknown, Unknown Region. 10.1088/1757-899X/186/1/012024 . hal-01694473

**HAL Id: hal-01694473**

**<https://hal.science/hal-01694473>**

Submitted on 14 Apr 2018

**HAL** is a multi-disciplinary open access archive for the deposit and dissemination of scientific research documents, whether they are published or not. The documents may come from teaching and research institutions in France or abroad, or from public or private research centers.

L'archive ouverte pluridisciplinaire **HAL**, est destinée au dépôt et à la diffusion de documents scientifiques de niveau recherche, publiés ou non, émanant des établissements d'enseignement et de recherche français ou étrangers, des laboratoires publics ou privés.

PAPER • OPEN ACCESS

## Synthesis, characterization and luminescent properties of $\text{Sr}_{1-x}\text{Pb}_x\text{WO}_4$ solid solution ( $x=0, 0.5$ and 1)

To cite this article: A Hallaoui *et al* 2017 *IOP Conf. Ser.: Mater. Sci. Eng.* **186** 012024

View the [article online](#) for updates and enhancements.

### Related content

- [Synthesis characterization and hydrogenation behaviour of as quenched  \$\text{Ti}\_{41.5}\text{Zr}\_{41.5}\text{XNi}\_{17}\$  \( \$x=0, 3.5, 11.5\$  and  \$13.5\$ \) nano quasicrystalline ribbons](#)  
Rohit R Shahi, T.P. Yadav, M.A. Shaz et al.
- [Luminescent properties of alumina ceramics doped with chromium oxide](#)  
V Kortov, A Kiryakov and V Pustovarov
- [LUNAR LUMINESCENCE](#)  
Robert L. Wildey

# Synthesis, characterization and luminescent properties of $\text{Sr}_{1-x}\text{Pb}_x\text{WO}_4$ solid solution ( $x=0, 0.5$ and $1$ )

A Hallaoui<sup>1,2</sup>, A Taoufyq<sup>1,2</sup>, B Bakiz<sup>2</sup>, F Guinneton<sup>1</sup>, J-C Valmalette<sup>1</sup>, S Villain<sup>1</sup>, M Arab<sup>1</sup>, A Benlhachemi<sup>2</sup>, L Bazzi<sup>2</sup> and J-RGavarri<sup>1</sup>

<sup>1</sup> IM2NP, UMR CNRS 7334, University of Toulon, BP 20132, 83957 La Garde-France

<sup>2</sup> LME, Faculty of Sciences, Ibn Zohr University, 80000 Agadir, Morocco

Email: abdelalihallaoui@gmail.com

**Abstract.** In this work, a study of the role of chemical substitution in the properties of the solid solution  $\text{Sr}_{1-x}\text{Pb}_x\text{WO}_4$  ( $x = 0, 0.5$  and  $1$ ) is presented. Polycrystalline samples were synthesized by solid state reaction at  $1100^\circ\text{C}$ . Using Rietveld method, the structural parameters of all samples were refined. All structures are of scheelite type. Scanning electron microscopy showed that a high level of crystallization characterized the samples, with modifications in sizes and shapes depending on composition  $x$ . The Infrared and Raman spectroscopies were performed to characterize the evolution of vibrational modes with composition  $x$ . Finally, a systematic study of luminescence under X-ray and UV excitations was performed. The energies and intensities of luminescence depended on composition  $x$  and on the nature of excitations.

## 1. Introduction

The first paragraph after a heading is not indented. The scheelite tungstate crystals  $\text{AWO}_4$  are characterized by tetragonal structures [1,2] (space group  $I4_1/a$ ), with tetrahedral oxyanions  $\text{WO}_4^{2-}$  and  $\text{M}^{2+}$  cations forming  $\text{MO}_8$  groups [3]. They were extensively investigated for their potential applications as laser host materials [4,5], scintillators [6,7], oxide ion conductors [8], materials for microwave applications [9] and magnetic materials [10]. The luminescent properties under different excitations of single-crystals as well as polycrystalline  $\text{SrWO}_4$  and  $\text{PbWO}_4$  compounds have been widely studied by several authors [11–15]. Generally, luminescence spectra of scheelite tungstate were decomposed into two main blue and green bands, and to a weaker orange–red emission: the emissions were observed with energies close to 3.0–2.8, 2.7–2.4 and 2.3–2.0 eV [16–20].

In this work we study the luminescent properties of lead and strontium tungstates  $\text{Sr}_{1-x}\text{Pb}_x\text{WO}_4$  for the three compositions  $x = 0 ; 0.5$  and  $1$  under X-ray and UV excitations. We already published the synthesis, characterization and luminescence under X-ray excitation of  $\text{Sr}_{1-x}\text{Pb}_x\text{WO}_4$  and  $\text{Ca}_{1-x}\text{Cd}_x\text{WO}_4$  solid solutions [21–23]. Presently, we compare the luminescence responses under X-ray and UV excitations of these substituted samples.

## 2. Experimental

### 2.1. Synthesis



All samples of  $\text{Sr}_{1-x}\text{Pb}_x\text{WO}_4$  with  $x=0, 0.5$  and  $1$ , were prepared by conventional solid state chemical reaction using  $\text{WO}_3$  [Alfa Aesar N° 11828, >99.8%],  $\text{SrCO}_3$  [Sigma-Aldrich N° 1633-05-2, >99.0%] and  $\text{PbO}$  [Sigma-Aldrich N° 1317-36-8, > 99.0%]. The elaboration conditions (grinding process, temperature and time of thermal treatment) were optimized and the final process was as follows: the reagents in stoichiometric proportions were thoroughly mixed and ground in an agate mortar for 15 min, then thermally treated at  $600^\circ\text{C}$  for 3 h, in pure alumina crucible under air. The samples were ground again thoroughly for 2 h, and then, retreated at  $1100^\circ\text{C}$  for 4 h, under air.

## 2.2. Characterization techniques

**2.2.1. X-ray diffraction:** Each sample was analysed by X-ray diffraction using an Empyrean Panalytical diffractometer, equipped with a copper X-ray source (wavelength  $\lambda=1.54.10^{-10}$  m, tension  $V=45$  kV, intensity  $I=35$  mA), and with a Ni filter eliminating the  $K_\beta$  radiation. The structural parameters of the samples were refined using the Fullprof software [24] based on Rietveld procedure.

**2.2.2. Scanning electron microscopy:** A systematic analysis of grain sizes and morphologies was performed using a Supra 40 V<sub>p</sub>Colonne Gemini Zeiss scanning electron microscope (SEM), with a maximum voltage of 20 kV.

**2.2.3. Raman spectroscopy analysis:** Raman spectroscopy was used to characterize the evolution of the various phases, and to correlate vibration modes with these structural evolutions. The equipment used to perform the various vibration spectra was a spectrometer Horiba Jobin-Yvon HR800 LabRam, spatially resolved to  $0.5\ \mu\text{m}$ , by means of an optical microscope with a 100 objective. The latter has a dual function: it allows firstly focusing the laser beam on a small area, and, secondly, visualizing the area of the sample. The 514.5 nm line of an Ar-ion laser was used as the excitation source; the photonic power applied to the samples was limited to  $5\ \mu\text{W}$  with an acquisition time of 30 s. Each Raman band was characterized by its wavenumber (in  $\text{cm}^{-1}$ ).

**2.2.4. Luminescence experiments:** For the luminescence under X-ray excitation, the copper X-ray source of the diffractometer Empyrean-Panalytical was used to irradiate the samples and perform luminescence experiments. The nominal emission conditions (voltage VRX / current IRX) were 45 kV /35 mA. The luminescence emissions of samples were recorded using a UV-visible spectrophotometer MicroHR (JobinYvon) equipped with an optical fiber of  $400\ \mu\text{m}$  in diameter.

The equipment used to perform the measurements of luminescence under UV was the previously described spectrometer Horiba Jobin-Yvon HR800 LabRam. The entrance slit, positioned behind the filter, is a diaphragm whose diameter can range from 50 to  $500\ \mu\text{m}$ . The 364.5 nm line of an Ar-ion laser was used as the excitation source. The power applied to the samples was fixed to 0.005 mW with an acquisition time set to 100 ms.

## 3. Results and discussion

### 3.1. X-ray diffraction

Fig. 1 shows the XRD pattern of  $\text{Sr}_{1-x}\text{Pb}_x\text{WO}_4$  powders. All diffraction peaks are characteristic of the scheelite tetragonal structure with space group  $I4_1/a$ . The diffraction peaks are shifted to smaller  $2\theta$  angles as  $x$  increases.

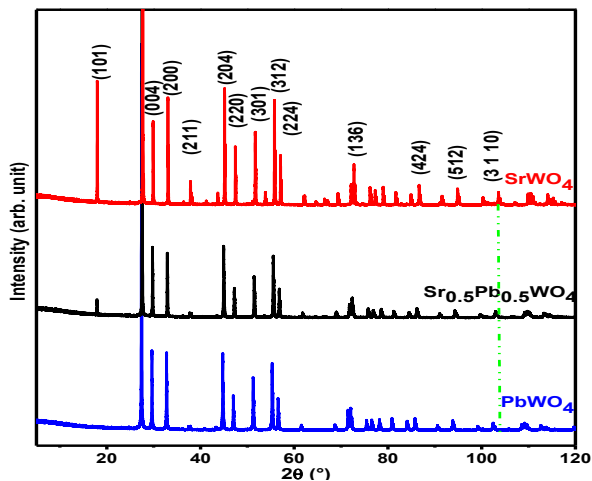


**Figure 1.** XRD patterns of the tetragonal  $Sr_{1-x}Pb_xWO_4$  powders with  $x = 0, 0.5, 1$ .

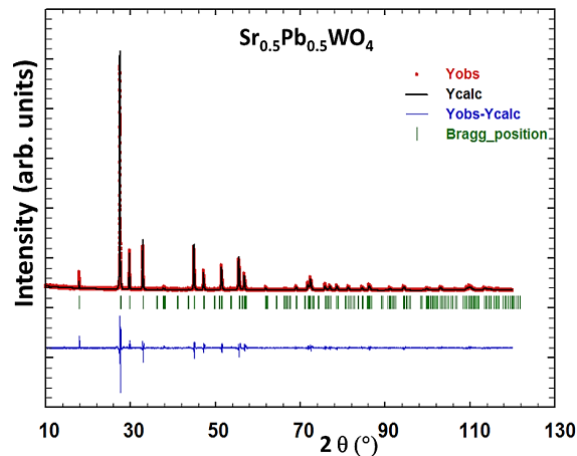


**Figure 2.** Calculated and observed diffraction profiles from Rietveld analyses for the  $Sr_{0.5}Pb_{0.5}WO_4$  phase.  $Y_{calc}$ : calculated profile and  $Y_{obs}$ : observed profile.

Table 1 reports the refined structural parameters. Fig. 2 shows selected results comparing calculated diffraction profiles to experimental data.

**Table 1.** Refined structural parameters for  $Sr_{1-x}Pb_xWO_4$  compounds with  $x = 0, 0.5, 1$ . Cell parameters, Debye-Waller factors B, reliability factors R in %.

<b>x</b>	<b>0</b>	<b>0.5</b>	<b>1.0</b>
a ( $10^{-10}$ m)	5.41734(2)	5.43919(3)	5.46220 (3)
b ( $10^{-10}$ m)	5.41734(2)	5.43919 (3)	5.46220 (3)
c ( $10^{-10}$ m)	11.95599(5)	11.99990(9)	12.04766(8)
Volume Cell ( $10^{-30}$ m <sup>3</sup> ): V	350.880(2)	355.014 (5)	359.450(4)
B (M) ( $8\pi^2/3$ ). $\langle\Delta r^2\rangle$ ( $\text{Å}^2$ )	0.37(3)	0.77(4)	0.38(2)
B (W) ( $\text{Å}^2$ )	0.21(3)	0.17(3)	0.20(2)
Reliability factors (*)			
R <sub>B</sub> %	5.53	7.64	7.01
R <sub>F</sub> (%)	5.34	7.24	8.04
R <sub>exp</sub> (%)	7.08	8.49	8.45
W (x,y,z)	Fixed values : x = 0.00000 ; y = 0.25000 ; z = 0.12500 (**)		
M (x,y,z)	Fixed values : x = 0.00000 ; y = 0.25000 ; z = 0.62500 (**)		
O (x,y,z)	Fixed values : x = 0.23880 ; y = 0.11410 ; z = 0.04290 (**)		

Notes :

(\*)  $R_B = 100 \cdot \left\{ \frac{\sum |I_k^{obs} - I_k^{calc}|}{\sum I_k^{obs}} \right\}$ ;  $R_F = 100 \cdot \left\{ \frac{\sum w_i |(I_{iobs})^{1/2} - (I_{ical})^{1/2}|}{\sum (I_{iobs})^{1/2}} \right\}$ ;  $R_{exp} = 100 \cdot \left\{ \left[ \frac{N - P}{\sum w_i |y_i^{obs}|^2} \right]^{1/2} \right\}$  where N, P are the number of observations and parameters respectively.

(\*\*) Sr, W and O coordinates from author [25] have been fixed.

### 3.2. Raman spectra

Fig. 3 shows the Raman spectra of the three compositions at room temperature. The vibration modes of  $SrWO_4$  and  $PbWO_4$  were already interpreted by authors *Priya et al.* and *Ling et al.* [26, 27] and

Crane *et al.* [28]. The decrease with composition  $x$  of Raman wavenumbers clearly suggests a continuous modification of chemical bonds W–O due to W–O–Pb interactions: as Pb–O bonds present a more covalent character, the W–O bonds probably present a weaker covalent character, with decreasing rigidity, due to electron displacement in favor of the Pb–O bond. In addition, a mass effect, due to a mass of Pb stronger than the mass of Sr, should play a role in the decrease of wavenumbers.

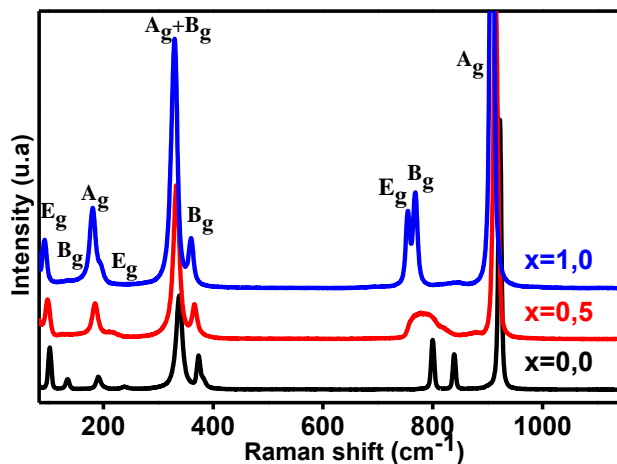


**Figure 3.** Room temperature Raman spectra of  $\text{Sr}_{1-x}\text{Pb}_x\text{WO}_4$ , for  $x = 0, 0.5, 1$ . ( $\lambda$  (excit.) = 514.5 nm).

### 3.3. Scanning electron microscopy

The SEM analyses of the  $x = 0.1, 0.5, 1$  samples (Figures 4a, 4b and 4c, successively) show a progressive increase of crystallite sizes as  $x$  increases. In Figure 4a, we have inserted a magnified image to better illustrate the morphologies. In the case of the  $x = 0.5$  sample (Fig. 4b), a majority of large and regular crystallites is observed. For  $\text{PbWO}_4$  (Fig. 4c) a mix system of crystallites with large and small grains is observed.

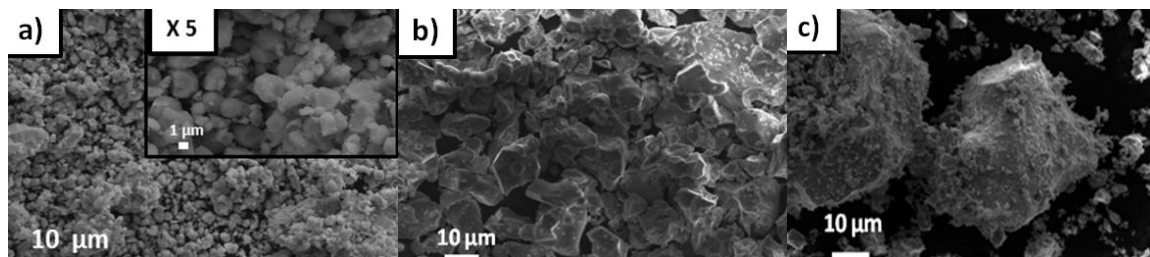


**Figure 4.** Scanning electron microscopy micrographs of the  $\text{Sr}_{1-x}\text{Pb}_x\text{WO}_4$  samples (a)  $x = 0$  In inset : magnification of image (a) ( $\times 5$ ), (b)  $x = 0.5$ , and (c)  $x = 1$ .

### 3.4. Luminescence under X-ray excitation

**Figure 5** compares the intensities emitted by the three different materials ( $x = 0, 0.5, 1$ ). We observe a clear difference between the intensity of the substituted compound ( $x = 0.5$ ) and those of  $x = 0$  and  $1$  samples, with a very strong intensity for the  $x = 0.5$  sample. The average energy of the emission band is close to 2.8 eV (blue region).

### 3.5. Luminescence under UV excitation

**Figure 6** shows the intensities of luminescence under UV excitation. In this case, no stronger intensity is observed for the substituted sample. This difference between the two emissions under UV and X-ray excitations can be ascribed to the low penetration of UV beam and to the high penetration of X-ray beam in samples. In the case of low energy UV excitation (3.6 eV), the observed luminescence is

mainly due to the external areas of crystallites and irregular surfaces of powdered samples, which is not the case for high energy X-ray excitations (from 0 to 45000 eV) that concern larger volumes of material. The average energy of the emission band is close to 2.25 eV (green region).

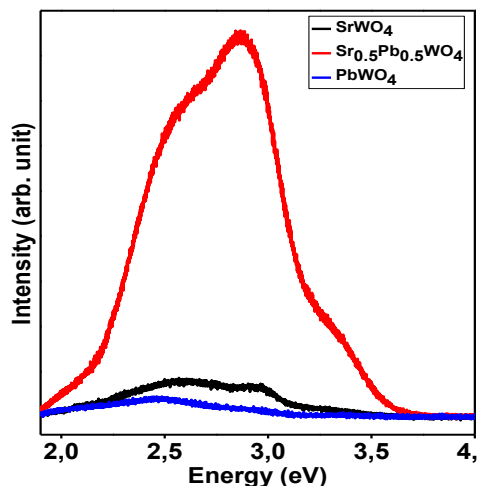


**Figure 5.** Photoluminescence spectra of SrWO<sub>4</sub>, Sr<sub>0.5</sub>Pb<sub>0.5</sub>WO<sub>4</sub> and PbWO<sub>4</sub> under X-ray excitation (excitation energies in the continuous range 0 to 45000 eV).

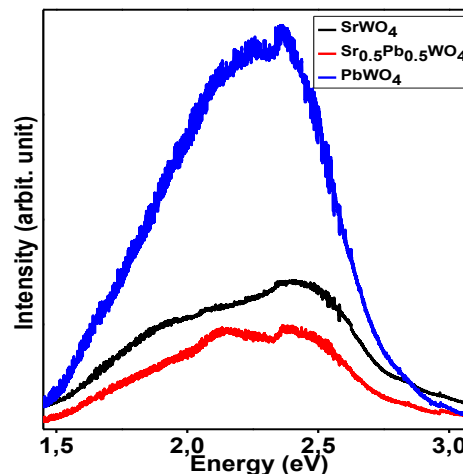


**Figure 6.** Photoluminescence spectra of SrWO<sub>4</sub>, Sr<sub>0.5</sub>Pb<sub>0.5</sub>WO<sub>4</sub> and PbWO<sub>4</sub> under UV excitation ( $\lambda = 364.5$  nm or  $E = 3.6$  eV).

#### 4. Conclusion

In this work, we have observed a complex influence of the chemical substitution on the luminescence signals under X-Ray excitation and UV excitation, in the series Sr<sub>1-x</sub>Pb<sub>x</sub>WO<sub>4</sub>. Generally the origin of the emission in tungstate materials is related to the classical  $^3T \rightarrow A_1$  transitions in the oxyanions WO<sub>4</sub><sup>2-</sup>, and cations or anions vacancies in the material. The emission energies under X-ray and UV excitations are in the blue and green regions respectively. The luminescence experiments under X-ray excitation show that the emission of Sr<sub>0.5</sub>Pb<sub>0.5</sub>WO<sub>4</sub> presents intensity stronger than the intensity observed in SrWO<sub>4</sub> and PbWO<sub>4</sub>. This behavior is fully different from the one observed in experiments under UV excitation: the emission intensity observed in the case of  $x=0.5$  sample is lowered in comparison with the one of SrWO<sub>4</sub> and PbWO<sub>4</sub>.

In these studies, we have shown that the effects of chemical substitution are complex, and that substitution can be used to obtain variable luminescence properties. The extension of these studies of substituted luminescent materials is now in progress: a major objective should be to better understand the different roles of substitution and of crystallization in luminescence efficiency.

#### Acknowledgments

This work was financially supported by the Regional Council of Provence-Alpes-Côte d'Azur (no. 2012-16322), by the General Council of Var and by Toulon Provence Mediterranean, and was conducted as part of the CNRS-CNRST 2014 project (Chimie 02/14).

#### References

- [1] Liao W, Wang Y-F, Liu Y-M., Li Y-D, Qian Y-T 2000 Chem. Mater. **12**2819.
- [2] Zhang Q, Yao W-T, Chen X, Zhu L, Fu Y, Zhang G, Sheng L, Yu S- H 2007 Cryst. Growth Des. **7**1423.
- [3] Gurman E, Daniels E, King J-S 1971 J. Chem. Phys. **55** 1093.
- [4] Treadaway M-J, Powel R-C 1975 Phys. Rev. B **11**862.
- [5] Chen W, Inagawa Y, Omatsu T, Tateda M, Takeuchi N, Usuki Y 2001 Opt. Commun. **194** 401.
- [6] Lecoq P, Dafinei I, Auffray E Nucl. 1995 Instrum. Methods **365**291.

- [7] TakaiS, SugiuraK, EsakaT1999Mater. Res. Bull.**34**193.
- [8] NagirnyiV, FeldbachE, OnssonL-J, KirmM, LushchikA, LushchikC, NagornayaL-L, RyzhikovV-D, SavikhiuF, SvenssonG, TupitsinaI-A1998Radiat. Meas. **29** 247.
- [9] Van-UitertL-G, Preziosi S1962 J. Appl. Phys. **33** 2908.
- [10] EhrenbergH, WeitzelH, HeidC, FuessH, WltschekG, Kroener T, Van-TolJ, BonnetM1997J. Phys.: Condens. Matter **9** 3189.
- [11] Van LooW1975Phys. Stat. Sol. A **27** 565.
- [12] Van LooW 1975Phys. Stat. Sol. A **28** 227.
- [13] BohacekP, ZazubovichS, SolovievaN, NiklM2007 Opt. Mat. **30** 66.
- [14] ChukovaO, NedilkoS2013 Opt. Mat. **35** 1735.
- [15] PôrtoS-L, LongoE, PizaniP-S, BoschiT-M, SimoesL-G-P, LimaS-J-G, FerreiraJ-M, SoledadeL-E-B, EspinozaJ-W-M, Cassia-SantosM-R, MaureraM-A-M-A, PaskocimasC-A, SantosI-M-G, SouzaA-G2008 J. Solid State Chem. **181** 1876.
- [16] BurachasS, BeloglovskyS, MakovI, SavelievYu, VassilievaN, IppolitovM, MankoV, NikulinS, VassilievA, ApanasenkoA, TamulaitisG2002Funct. Mater. **9** 297.
- [17] Kim T, Hole D-E, Townsend P-D, WooJ, WhangC 2005 Phys. Stat. Sol. c**2** 564.
- [18] LagutaV-V, NiklM, ZazubovichS IEEE Trans. Nucl. Sci.2008**55** 1275.
- [19] BurachasS, ApanasenkoA, GrinyovB, RyzhikovV, KatrunovK, StarzhinskiyM, IppolitovM, MankoV, TamulaitisG2001Int. J. Inorg. Mater. **3** 1101.
- [20] NovosadS-S, KostykL-V, NovosadS-I 2011 J. Appl. Spectrosc. **78**557.
- [21] Hallaoui A, Taoufyq A, Arab M, Bakiz B, Benlhachemi A, Bazzi L, Villain S, ValmaletteJ-C, GuinnetonF, GavarrriJ-R2015J. of Sol. St. Chem. **227** 186.
- [22] Taoufyq A, Guinneton F, Valmalette J-C, Arab M, Benlhachemi A, Bakiz B, Villain S, LyoussiA, NolibeG, GavarrriJ-R 2014 J. of Sol. St. Chem. **219**127.
- [23] Taoufyq A, MauroyV, GuinnetonF, BakizB, VillainS, HallaouiA, BenlhachemiA, NolibeG, LyoussiA, GavarrriJ-R 2015 Mater. Res. Bull.**70** 40.
- [24] RoisnelT, Rodríguez-CarvajalJ, DelhezR, MittenmeijerE-J 2000(Eds.)Proceedings of the Seventh European Powder Diffraction Conference, Barcelona 118.
- [25] PecharskyV-K, ZavalijP-Y 2005 Springer Science & Business Media 512.
- [26] PriyaA, SinhaE, RoutS-K 2013 Solid State Sc. **20** 40.
- [27] LingZ-C, XiaH-R, RanD-G, LiuF-Q, SunS-Q, FanJ-D, ZhangH-J, WangJ-Y, YuL-L 2006 Chem. Phys. Lett. **426** 85.
- [28] CraneM, FrostR-L, WilliamsP- A, KloproggeJ-T 2002 J. Raman Spectrosc. **33** 62.